Journal of Power Sources 184 (2008) 288–296

Contents lists available at ScienceDirect

Journal of Power Sources

journal homepage: www.elsevier.com/locate/jpowsour

# Effect of zwitterion on the lithium solid electrolyte interphase in ionic liquid electrolytes

N. Byrne[a,1,2], P.C. Howlett[a,1], D.R. MacFarlane[b,1], M.E. Smith[c], A. Howes[c], A.F. Hollenkamp[d], T. Bastow[e], P. Hale[f], M. Forsyth[a,*,1]

[a] Department of Materials Engineering, Monash University, Wellington Road, Clayton 3800, Vic., Australia
[b] School of Chemistry Monash University, Wellington Road, Clayton 3800, Vic., Australia
[c] Department of Physics, Warwick University, Coventry, UK
[d] CSIRO Energy Technology, Box 312, Clayton South, Vic. 3169, Australia
[e] CSIRO Manufacturing and Materials Technology, Box 312, Clayton South, Vic. 3169, Australia
[f] Department of Physics, La Trobe University, Vic. 3086, Australia

ARTICLE INFO

*Article history:*
Received 11 January 2008
Received in revised form 12 March 2008
Accepted 16 April 2008
Available online 21 May 2008

*Keywords:*
Solid electrolyte interphase
Zwitterion
Current density
Lithium-metal battery
Nuclear magnetic resonance

ABSTRACT

An understanding of the solid electrolyte interphase (SEI) that forms on the lithium-metal surface is essential to the further development of rechargeable lithium-metal batteries. Currently, the formation of dendrites during cycling, which can lead to catastrophic failure of the cell, has mostly halted research on these power sources. The discovery of ionic liquids as electrolytes has rekindled the possibility of safe, rechargeable, lithium-metal batteries. The current limitation of ionic liquid electrolytes, however, is that when compared with conventional non-aqueous electrolytes the device rate capability is limited. Recently, we have shown that the addition of a zwitterion such as *N*-methyl-*N*-(butyl sulfonate) pyrrolidinium resulted in enhancement of the achievable current densities by 100%. It was also found that the resistance of the SEI layer in the presence of a zwitterion is 50% lower. In this study, a detailed chemical and electrochemical analysis of the SEI that forms in both the presence and absence of a zwitterion has been conducted. Clear differences in the chemical nature and also the thickness of the SEI are observed and these may account for the enhancement of operating current densities.



## 1. Introduction

Rechargeable lithium-metal batteries represent the future for portable technology. The high theoretical specific energy of metallic lithium [1,2] is the main driver for the development of safe, rechargeable, lithium-metal batteries. A major limitation in the development of these devices is the problem of dendrite growth [3,4], which can lead to catastrophic failure. Dendrite growth and other limitations such as poor cycle and shelf life, all stem from the development of an electrically insulating layer on the both the negative (anode) and positive (cathode) electrodes. This is known as the solid electrolyte interphase (SEI) [5,6]. It is now well understood and accepted that the formation of a suitable SEI is critical to the successful operation of a lithium battery.

The SEI that forms is thought to be the product of many factors but generally the composition is dominated by reactions with various components of the electrolyte [7,8]. To improve the properties of the SEI, various additives such as benzene or toluene which are known to cover the lithium surface and limit reaction between the surface and the electrolyte [9] have been tried.

It has been shown recently [10–13] that the use of ionic liquids (ILs) as electrolytes in lithium cells is successful in suppressing dendrite formation at low cycling rates. Ionic liquids are emerging as potentially excellent replacement electrolytes for traditional volatile electrolytes in many electrochemical devices and other processes [14–19]. This is due to the many favourable properties that are typical of ionic liquids, namely, a large electrochemical window (in some cases, exceeding 6 V), liquid across a wide range of temperatures, effectively zero volatility and flammability, and high conductivity [16,18,20]. It is thought that due to mass-transport limitations in the electrolyte, higher and more practical cycling rates cannot be achieved with present ionic liquid electrolytes.

* Corresponding author. Tel.: +61 3 9905 4939; fax: +61 3 9905 4940.
*E-mail addresses:* Patrick.Howlett@csiro.au, Maria.Forsyth@eng.monash.edu.au (M. Forsyth).
[1] ARC Centre of Excellence for Electromaterials Science.
[2] Current address: Department of Chemistry and Biochemistry, Arizona State University, Tempe 85287, AZ, USA.

0378-7753/$ – see front matter. 
doi:10.1016/j.jpowsour.2008.04.094

Recently, we have shown [22] that the addition of zwitterionic compounds can increase the diffusivity of the lithium ion and can, in practice, result in a 100% increase in the rate capability of a symmetrical lithium cell. In that work, it was found [23] that the resistance of the SEI was reduced by 50% with zwitterion addition. Importantly, it is thought that the addition of a zwitterion will not alter the attractive properties of the ionic liquid electrolyte.

An understanding of the SEI would hold a key towards the further development of safe, rechargeable, lithium-metal batteries. A model has been developed [24] of the SEI layer that forms in a lithium-metal battery when an ionic liquid similar to that used in this study is cycled. It was proposed that the SEI was multilayered. The innermost layer, closest to the lithium-metal surface, contained LiF and $Li_2O$; the latter is presumably present, at least in part, due to the native lithium surface. The next layer was identified as LiF in majority, whilst the outermost layer contained numerous breakdown products of the electrolyte. It was proposed that this breakdown layer was, in relative terms, the thinnest and most insulating.

This work examines the SEI that forms on lithium metal when using an electrolyte consisting of 0.5 mol $kg^{-1}$ of lithium bis(trifluoromethanesulfonyl)amide in *N*-methyl-*N*-propyl pyrrolidinium bis(trifluoromethanesulfonyl)amide [$C_3$mpyr][$NTf_2$] with and without the addition of a zwitterion (0.15 mol $kg^{-1}$ *N*-methyl-*N*-(butyl sulfonate) pyrrolidinium). The chemical structures of these materials are shown in Fig. 1. The information obtained from solid-state nuclear magnetic resonance (NMR), X-ray photoelectron spectroscopy (XPS) and electrochemical techniques indicates that the addition of the zwitterion leads to a thinner SEI overall and fewer electrolyte breakdown products in the outermost layer.

## 2. Experimental

### 2.1. Synthesis

The room temperature ionic liquids (RTILs) and zwitterion used in the study were synthesized according to the procedure described in earlier publications [22,29]. The electrolytes were prepared by adding 0.5 mol $kg^{-1}$ of lithium bis(trifluoromethanesulfonyl)amide to *N*-methyl *N*-propyl pyrrolidinium bis(trifluoromethanesulfonyl)amide. The 'with zwitterion' electrolytes were prepared by the further addition of 0.15 mol $kg^{-1}$ *N*-methyl-*N*-(butyl sulfonate) pyrrolidinium zwitterion. The electrolytes were heated in a vacuum oven at 65 °C for 12 h and degassed overnight with a stream of argon gas to ensure complete removal of water and dissolved gases.

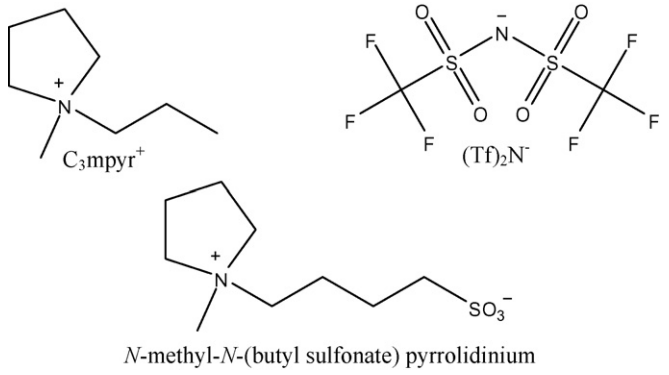


**Fig. 1.** Chemical structures of ionic liquid *N*-methyl-*N*-propyl pyrrolidinium bis(trifluoromethanesulfonyl)amide [$C_3$mpyr][$NTf_2$] and zwitterion (*N*-methyl-*N*-(butyl sulfonate) pyrrolidinium).

### 2.2. Lithium deposition

A charge of 5 C of lithium metal was deposited on to a copper substrate at a rate of 0.1 mA $cm^{-2}$. Sealed stainless steel cells were used to simulate battery conditions. The cells were fabricated from 316 stainless steel and consisted of two half 'cups'. The two halves were separated by a Teflon spacer that also served to seal the cell. Inside the cell, a stainless-steel piston on a spring within a polyvinyl chloride sleeve provided the stack pressure (~1 kg $cm^{-2}$). The electrodes were formed by cutting lithium foil (Aldrich 99.9%, thickness 180 μm) with a 1.6 cm diameter stainless-steel punch, to give an electrode area of 2 $cm^2$. A glass-fibre separator (Whatman GF/A type) was used to insulate the two electrodes. The lithium symmetrical cells were assembled in an argon-filled glove-box prior to removal for study. Cell cycling was performed by means of a Princeton Applied Research VMP2/Z potentiostat. At the conclusion of the deposition phase, galvanostatic cycling of the cells was conducted according to the method detailed below.

### 2.3. Cycling

Galvanostatic cycling was performed with a Battery Test Unit 1470 interfaced to a Solartron 1256 FRA that used Corrware (version 2.7) from Scribner Associates. Electrochemical impedence spectroscopy measurements were obtained from 100 kHz to 0.1 Hz with an amplitude of 5 mV versus the open-circuit voltage (OCV). Surface characterisation (NMR and XPS) was undertaken on the cycled lithium surface (40 cycles at 0.1 mA $cm^{-2}$) deposited on the copper substrate.

### 2.4. Nuclear magnetic resonance (NMR)

$^7$Li linewidth measurements were conducted with a Chemmagnetics 600 spectrometer that was operated at a frequency of 233.255 MHz. Pulse lengths of 3 μs were used with a recycle delay of >5$T_1$. For all spectra shown, 64 scans were collected at 25 °C. A spinning speed of 22 kHz was used to resolve the peaks. LiCl served as the reference standard at a concentration of 1 mol $L^{-1}$. Rotor preparation entailed scraping all of the products from the copper electrode surface and combining them with $SiO_2$ powder. Thus the spectra were expected to show peaks that belong to both the electrolyte and the lithium metal. This method ensured that the SEI constituents were not modified by the use of cleaning solvents. All rotor preparations were performed in an argon drybox.

### 2.5. X-ray photoelectron spectroscopy (XPS)

Spectra were acquired with a Kratos Axis, ultra imaging, XPS spectrometer. An aluminium monochromated X-ray source operating at 10 mA and 15 kV was focused on the sample surface. Survey spectra were acquired at a 160-eV pass energy, whereas high-resolution region spectra were obtained at a 20-eV pass energy.

Etching experiments were performed on the sample surface at varying etching lengths (stated in the paper depending on the surface). The estimated etching speed of the focused argon ion beam operating at 15 mA and 5 kV was approximately 1 Å $s^{-1}$. Instrument operation and peak fitting were performed using XPS AXIS ultra software. A 70:30 Gaussian:Lorentzian algorithm was applied to fit the peaks to obtain quantitative results. Samples were loaded into the instrument under argon and analysis was performed in a vacuum of $1.2 \times 10^{-8}$ Torr.

## 3. Results

### 3.1. Preparation of SEI surface

The galvanic deposition curve of lithium metal on a copper substrate is shown in Fig. 2. This curve can be divided into two sections that reflect two processes: the formation of the SEI and the subsequent steady-state deposition of lithium metal. The initial section of the curve is shown in more detail in the insert. A two-step process occurs and this may be linked to the breakdown of electrolyte components that lead to the formation of the SEI [21,24]. Following this, a plateau close to 0 V versus a $Li/Li^+$ reference electrode indicates the deposition of lithium metal from the electrolyte. Ideally, metal deposition should take place at 0 V (versus Li) but the internal resistances of the cell leads to a slight negative plating potential. In the electrolyte containing the zwitterionic species, the deposition is closer to 0 V (versus Li) and occurs at approximately −100 mV, as opposed to −200 mV in the absence of the zwitterion. This indicates that the total resistance in the cell containing the zwitterion is less. It is also significant that, in the absence of the zwitterion, the time taken to build the SEI (taken from the section of the graph shown in the insert) is longer than in the presence of zwitterion. This time can be quantified as representing the amount of charge that is consumed in the 'building' stage. This can be calculated from the point where the curve forms a plateau (as shown in Fig. 2 and indicated by the arrows). The charge required for the zwitterion containing electrolyte was 22 mC, compared with the neat system which consumed 43 mC.

The next step in the preparation of the electrode surface was to subject the cell to 40 cycles at a constant rate (0.1 mA $cm^{-2}$) and at room temperature. The cycling profile for the 'with' and 'without' zwitterions-containing electrolyte is shown in Fig. 3. If these cells are taken to be symmetrical lithium-metal cells (given that one side is lithium metal and the other is 5 C of lithium metal deposited on a copper substrate) the voltage reached during any cycle should be close to 0 V (versus Li). In practice, however, overpotentials occur, as already highlighted. It can be seen from Fig. 3a that the electrolyte containing the zwitterion operates at lower overpotentials throughout the 40 cycles when compared with the electrolyte without the zwitterion. This has been reported in an earlier study [25], in which it was shown that a cell containing the zwitterion was capable of sustaining double the current density of a cell without the zwitterion before cell failure occurred.

The cell containing the IL/Li salt electrolyte exhibits increasing overpotential with increasing cycle number (time). The impact of this cycling on the SEI resistance can be seen in Fig. 3b, which shows the impedance plots of both cells, with and without zwitterion addition, before and after cycling. The first intercept represents the electrolyte resistance, whereas the second intercept represents the resistance of the SEI. The cell containing zwitterion shows very little change in the resistance of both the electrolyte and the SEI before and after cycling. In fact, the resistance decreases slightly. By contrast, in the absence of zwitterion significant changes occur; in particular, the resistance of the SEI increases considerably after cycling. It can be seen that the resistance of the SEI before cycling is less when the zwitterion is present, compared with the electrolyte without zwitterion. This can account for the higher overpotentials seen in the cycling profile, and provides further evidence of the importance of the SEI for cell performance and the effect of a zwitterion upon it.

### 3.2. Solid-state NMR characterisation of SEI layer

The lithium environment of the SEI layer was investigated using high-resolution NMR. This allows the possible lithium species, which may be present in the SEI, to be identified. The $^7Li$ linewidth spectrum for the electrolyte surface taken from the zwitterion cell is shown in Fig. 4. The sweep width in this figure is large to take into account the 265 ppm Knight shift of lithium metal. Lithium metal

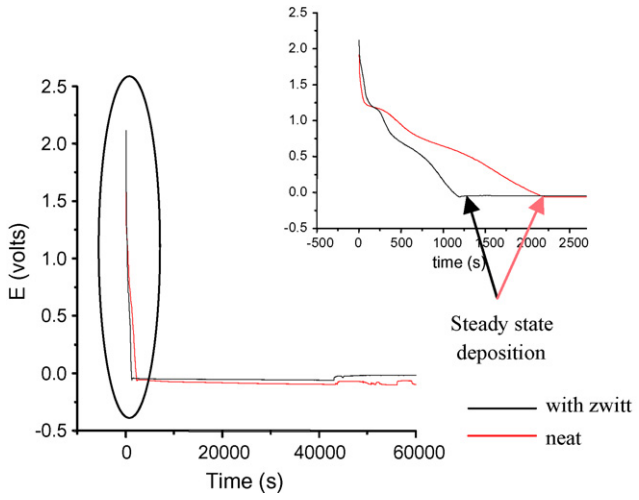


**Fig. 2.** Deposition curve for samples with and without zwitterion. Insert highlights the initial section of curve. Arrows highlight start of steady-state lithium deposition for the two samples (neat = without zwitterion).

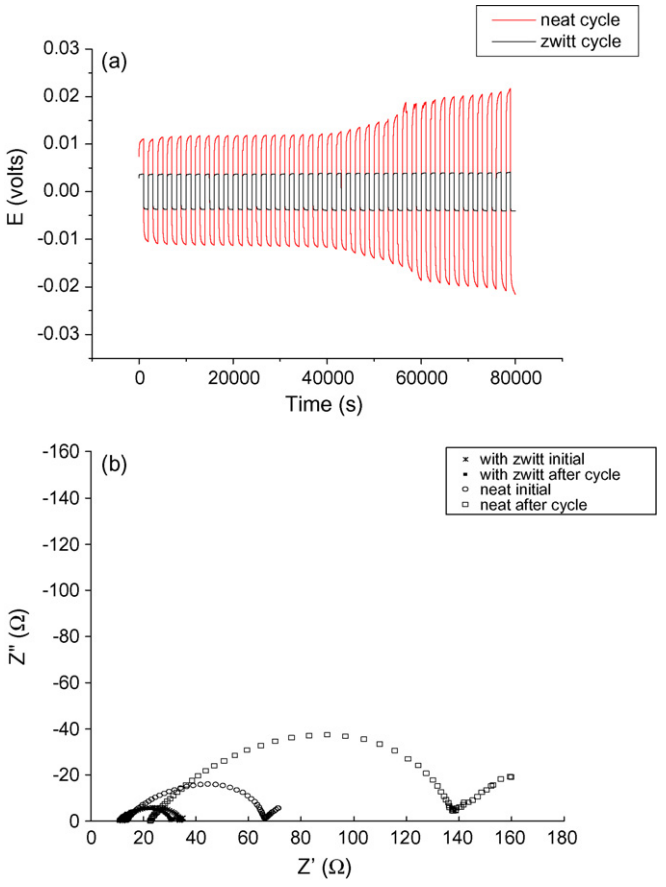


**Fig. 3.** (a) Cycling profile for samples with and without zwitterion. (b) Impedance data obtained for both samples (with and without zwitterion) before and after cycling.

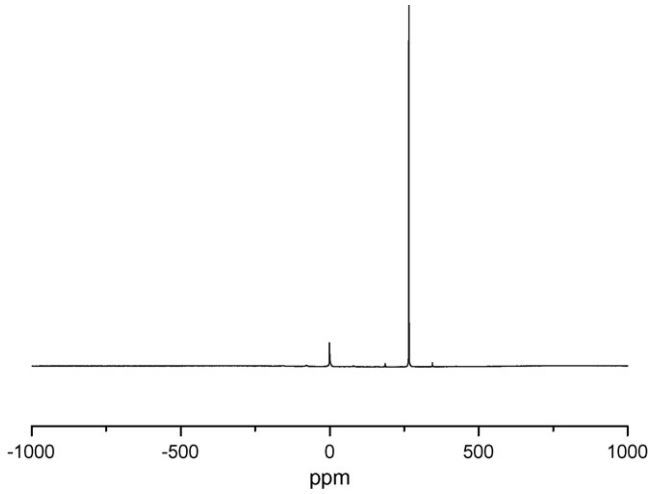


**Fig. 4.** $^{7}$Li spectra taken over large spectral width to identify metallic lithium as well as inorganic lithium species in case of Li metal cycled in the IL and zwitterion electrolyte.

is present in the spectrum, as expected given the rotor preparation (see Section 2). At this large sweep width, very few differences are apparent between the two surfaces and only the zwitterion spectrum has been shown for clarity.

At a reduced sweep width, clear differences between the two spectra become evident. The $^{7}$Li spectrum of the sample with and without the zwitterion overlaid on the same ppm scale (reference to 1 M LiCl) is presented in Fig. 5. The SEI formed in the absence of the zwitterion displays three peaks. The peak at around 0 ppm can be assigned to the electrolyte (as measured). To assign the other peaks, the chemical shift library of $^{7}$Li inorganic compounds published by Greenbaum and coworkers [26] was utilized with the addition of $Li_2S$ with a chemical shift of 1.6 ppm. LiF was shown by Greenbaum to have a chemical shift of −1 ppm, from which it can be concluded that the peak on the spectrum without the zwitterion at −1 ppm can be assigned to LiF. The large broad peak appearing positive of 0 ppm, according to the library of inorganic compounds, can be assigned to either $Li_2CO_3$ or $Li_2O$ species. Comparing this with the spectrum obtained in the presence of the zwitterion, it can be seen that only two distinct peaks are present. Again, there is a broad component appearing positive of 0 ppm. With a zwitterion, however, the intensity of the peak is less, which indicates that less of this component

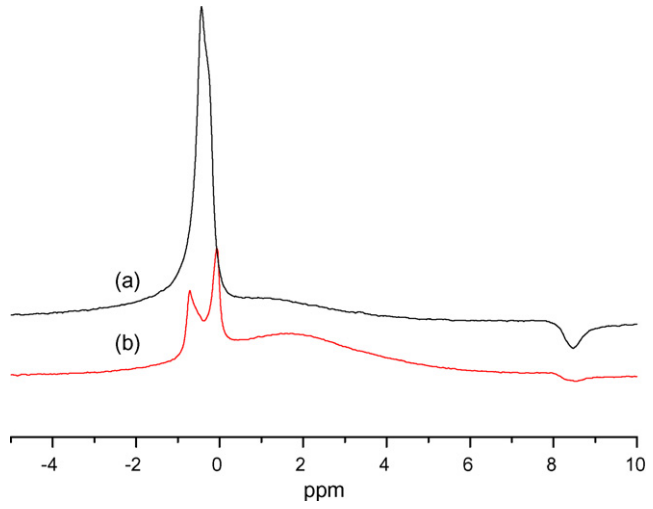


**Fig. 5.** $^{7}$Li MAS spectra for samples with (a) and without (b) zwitterion.

is present. The sample amounts in this experiment were carefully weighed, therefore intensity is a direct measurement of the amount and comparisons to that effect are valid. Also, the chemical shift is different, which suggests that the main lithium salts contributing to this peak are $Li_2S$ and/or LiOH compounds. Given that it has been shown [2] that the breakdown layer is comprised mainly of lithium salts from the ionic liquid anion it appears that, with the addition of a zwitterion, less 'breakdown' lithium salts are produced with the chemical nature of these salts differing. For the zwitterion-containing spectrum, the peak appearing at around 0 ppm does not resolve into two peaks as readily as in the absence of the zwitterion. On the other hand, the broadness of the peak is similar to the two peaks in the without zwitterion case. This indicates that either a smaller amount of LiF exists or, more likely, the electrolyte and the LiF are interacting more intimately in the presence of the zwitterion. It is therefore concluded that little to no breakdown layer exists, which will also be shown in the following section.

### 3.3. XPS characterisation of SEI

X-ray photoelectron spectroscopy is an attractive technique for determining surface layer composition and structure because of its ability to distinguish between different oxidation states. In addition, etching with an argon ion beam allows inner layers to be revealed. It should be noted, however, that this process is destructive and can alter the sample composition and hence any detailed chemical modelling should be supported by other techniques.

High-resolution region spectra were acquired for the initial surface, at etching times of 8, 16 and 24 min for the zwitterion-containing surface, and at etching times of 8 and 16 min for the neat IL surface. A summary of the results for the F 1s high-resolution data for both surfaces is presented in Fig. 6. The initial spectrum in both cases has a similar appearance and shows two peaks identified as $CF_3$ at 688.7 eV and LiF at 685 eV. There is a significant amount of $CF_3$ present on both surfaces, presumably from the ionic liquid, together with a very small amount of LiF. The 8-min etch spectra of both surfaces show dramatic differences. In the zwitterion case, the 8-min F 1s spectra is dominated by LiF, showing large quantities of this species and almost no $CF_3$, compared with the neat IL surface where both species are present in similar amounts. The 16-min etch spectra of both surfaces appear very similar with LiF being the majority species present. It can be concluded that as the etching time is increased, the amount of $CF_3$ decreased in both cases. Further, it is hypothesised that the $CF_3$ species make up the breakdown layer in part, and that etching this layer reveals the compact LiF layer. In the zwitterion case, LiF quickly dominates the surface whereas in the absence of zwitterion a more steady change occurs and provides another indication that the SEI layer without zwitterion may be thicker. Also, if a comparison is made of the atomic concentrations of the different F 1s species present on both surfaces, it is interesting to note that the total amount of LiF in the zwitterion-containing surface is less.

A summary of the data obtained for the S 2p photoelectron line is presented in Fig. 7. Again, the initial spectra look very similar for both surfaces: two doublets are present arising from spin orbit splitting of the S 2p photoelectrons; the dominant peaks appear at 166.7 eV (identified as $–SO_2$) and 168.5 eV (identified as $–SO_2CF_3$). These can be attributed to breakdown products of the ionic liquid anion [21,24]. After the 8-min etch, the spectra show clear differences between the two surfaces. In the case of the without zwitterion surface, four sulfur species are identified; the major sulfur component is the breakdown product $–SO_2CF_3$. When compared with the 8-min etch of the surface containing the zwitterion, four sulfur-containing species are again identified, but the major

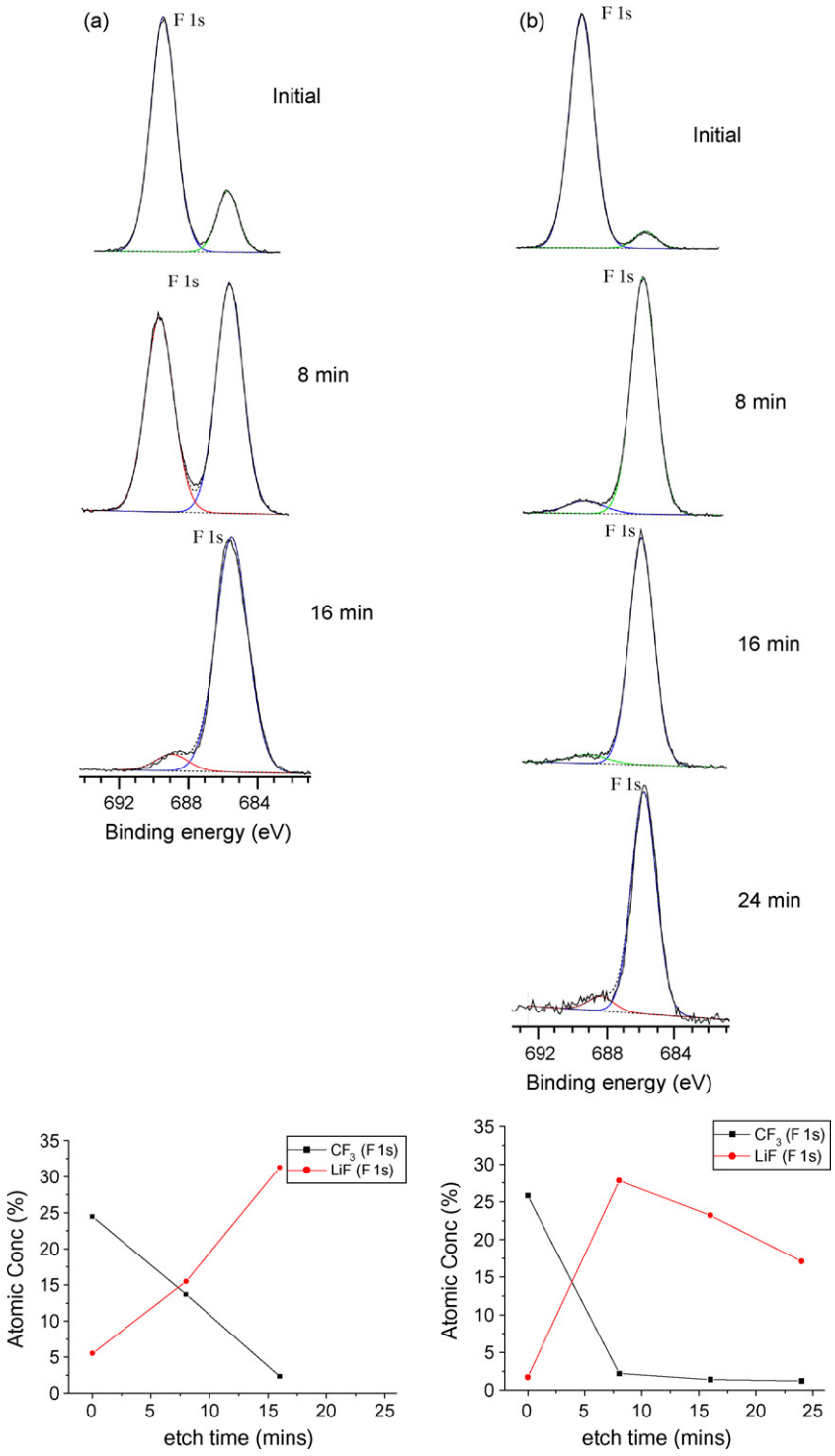


**Fig. 6.** High-resolution F 1s region spectra and atomic concentrations as function of etch time for (a) without zwitterion and (b) with zwitterion.

sulfur species appears to be $S^{2-}$. This again supports the $^{7}Li$ NMR data, which indicates that the zwitterion surface is rich in $Li_2S$. Comparing the atomic concentration as a function of etch time for both surfaces shows that the total amount of sulfur species present is higher for the neat surface, and although the trend appears similar it can be seen that even the 16-min etch spectra are different. These differences in sulfur species may account for the differences seen in the resistances, as $Li_2S$ is a favourable SEI product being itself a good lithium-ion conductor. Therefore, even small amounts of this compound in the SEI may make a significant contribution to the observed differences in the resistance of the two surfaces.

The differences observed for N 1s species on the two surfaces are highlighted in Fig. 8. Two species were identified; the $N^-$ at 403 eV and the $N^+$ at 398 eV. In particular, the excess of the $N^+$ is further evidence for an outermost layer consisting of electrolyte breakdown products; presumably the cation is present as precip-

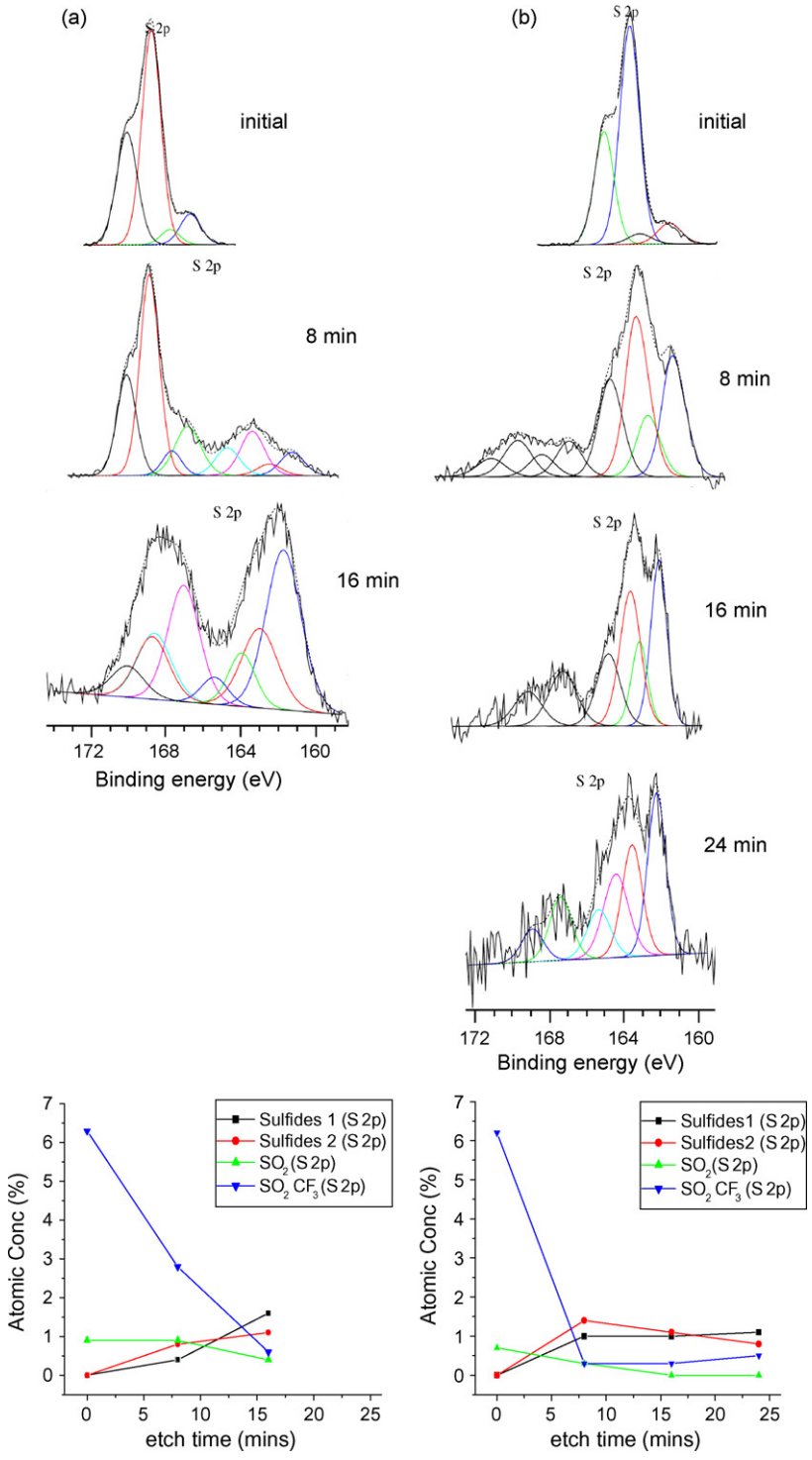


**Fig. 7.** High-resolution S 2p data region spectra and atomic concentration as function of etch time for (a) without zwitterion and (b) with zwitterion.

itated salts of reduced anion components. The initial spectra for both samples appear similar although the ratio of $N^+$:$N^-$ is greater for the zwitterion surface (i.e., ~2.2:~1.6). Clear differences are evident between the two samples after 8-min etching. In the without zwitterion surface, both the $N^+$ and $N^-$ species are still present. Howlett et al. [24] reported similar results, based on the same conditions for an electrolyte without zwitterion, suggesting that the $[C_3mpyr]^+$ was trapped within the different surface layers. When zwitterion is present, however, the $N^+$ peak (occurring at 403 eV) is mostly absent. This not only supports a thinner breakdown layer but furthermore, given that the amide is always present for the neat spectra at all etch depths, this suggests that the breakdown reactions, and therefore products, may differ in the presence of the zwitterion. The other difference is the presence of a new N 1s species for the zwitterion surface. The peak occurs at a binding energy of 400.5 eV and, consequently, it is thought to be associated

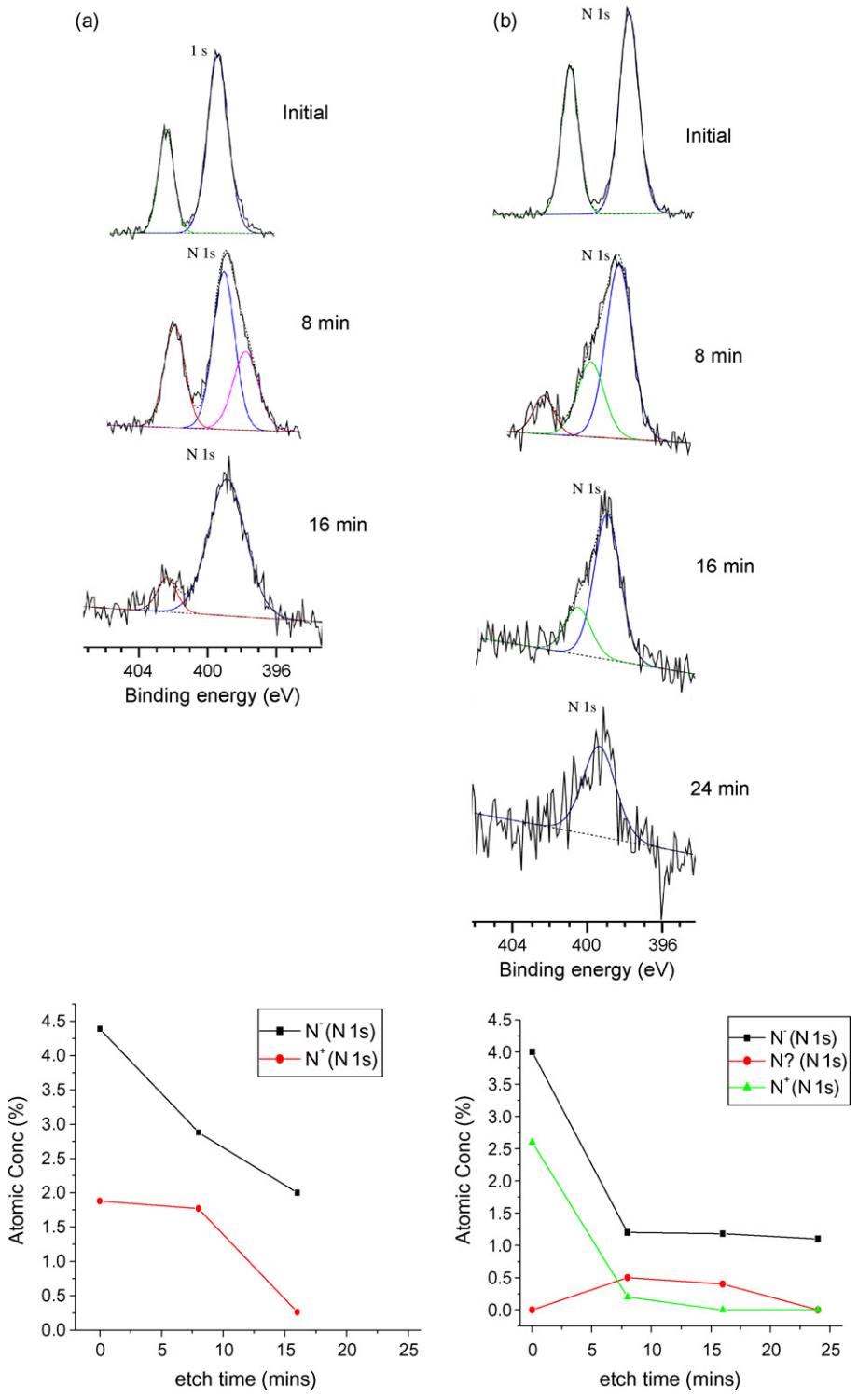


**Fig. 8.** N 1s region spectra and atomic concentration as function of etch time for (a) without zwitterion and (b) with zwitterion.

an amide-type product. This N 1s peak may in fact belong to the cation moiety of the zwitterion, given that it is not present in the neat IL spectrum.

Another indication that the relative thickness of the SEI in the two systems is different is shown in Fig. 9, which shows the atomic concentration of Cu acquired from survey spectra as a function of etch time. Substantial amounts of copper (i.e., >10 wt.%) are exposed on the zwitterion surface after 10–15 min of etching, whereas only small quantities are evident on the without zwitterion surface. This is also supported by data obtained by Howlett et al. [24], which show similar quantities of copper appearing after 40 min of etching. This is only indicative given that such a small area is etched, but when additional evidence from both the electrochemical and NMR experiments is taken into account there are strong indications that, in the presence of the zwitterion, the overall layer is thinner.

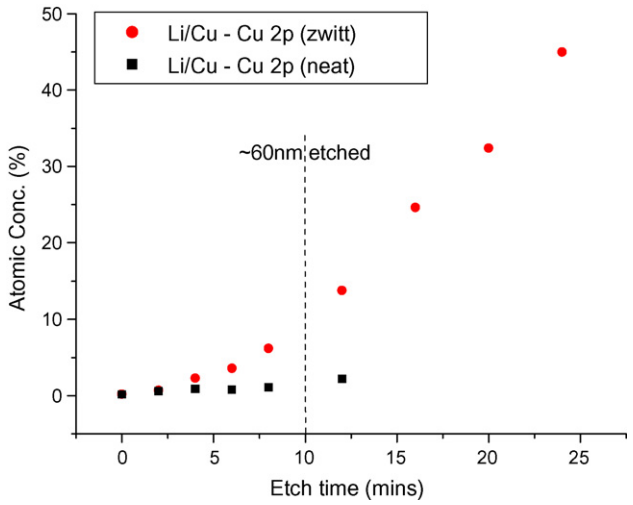


**Fig. 9.** Atomic concentration as a function of etch time for both with and without zwitterion surfaces. Point at which ~60 nm of material is etched indicated on graph; this is where copper is largely exposed on zwitterion surface.

## 4. Discussion

It has been proposed by several authors [6,27] that the SEI formed on lithium and lithium-loaded electrode surfaces is multi-layered in nature; Eshkenazi et al. [27] have broken the transport processes in the SEI into three main steps: electron transfer at the metal|SEI interface, migration of ion species from one interface to another, and transfer at the SEI|solution interphase.

The layer that forms closest to a metal surface is generally comprised of more heavily reduced species. This is observed in the present work and is supported by XPS data, which show a high concentration of LiF and $Li_2O$ as the etch time is increased. It is proposed that this inner layer forms rapidly and as such contains a high degree of defects that lead to high conductivity. The layer furthest away from the lithium metal anode, i.e., the outer layer, generally contains less reduced species and forms at a slower rate; thus this layer is expected to be less conductive. Howlett et al. [24] have described this outer layer as the 'breakdown' layer as it is comprised mainly of electrolyte breakdown products, in particular breakdown products of the $[NTf_2]^-$ anion. The breakdown layer is described as an insulator, as it has higher resistance relative to the inner layer and therefore does not as readily facilitate lithium transport.

The formation of a thinner SEI layer and the absence of $N^+$ in the layer close to the metal surface when the IL electrolyte also contains the zwitterion may be reconciled as follows. Although the delocalized charge of $[NTf_2]^-$ is well known and makes Li $[NTf_2]$ an attractive lithium salt in battery electrolytes from an ion dissociation point of view, relatively strong interactions can still occur between the Li and the $[NTf_2]^-$ anion. Li···$[NTf_2]$ co-ordination has been confirmed by Raman spectroscopy [28], thus accounting for the high degree of ion dissociation in an IL electrolyte without a zwitterion. The charge on the zwitterion is much more localized, perhaps due to the long alkyl chain, and the lithium ion may therefore co-ordinate with the zwitterion in preference to the $[NTf_2]^-$ anion. Consequently, the concentration of the $[NTf_2]^-$ anion at the electrolyte|electrode interphase may be reduced relative to the case when no zwitterion is present. As less $[NTf_2]^-$ anion breakdown products exist due to a lower concentration of $[NTf_2]^-$ at this electrode|electrolyte interphase, this could explain the thinner SEI layer.

The other difference observed is the absence of $N^+$ species, assumed to be $C_3mpyr^+$ species, in the inner layer. The addition of a zwitterion has previously been shown to increase the $^7Li$ diffusion coefficient by a factor of two [23]. Accordingly, even under the initial extreme potential required for in situ deposition, the supply of lithium ions to the electrode and thus the availability of lithium to react to form lithium-containing SEI products is greater due to an increase in lithium ion mobility. In summary, zwitterion assists in the formation of a thinner, inorganic lithium dominated film by: (i) allowing more rapid transport of $Li^+$ to the reactive electrode relative to the pyrrolidinium cations; (ii) decreasing the relative concentration of $[NTf_2]^-$, which results in less entrapment of organic species.

Fig. 10 shows a schematic view of the SEI layer proposed by Howlett et al. [24] and modified according to the XPS and NMR data presented for surfaces in the absence and presence of a zwitterion, respectively. First, the total thickness of the SEI layer formed in the presence of a zwitterion is represented as being considerably thinner. This alone could account for the higher current densities obtained with a zwitterion. Given the hypothesis that cell rate limitations are linked to ion movement through this layer, then a thinner layer will result in better cell performance. The other major difference is the presence of $N^+$ in the XPS spectra of the surface without a zwitterion. Howlett et al. [24] also observed this for lithium metal deposited on copper, but not for a native lithium surface. The plating of lithium metal on to a copper substrate is a

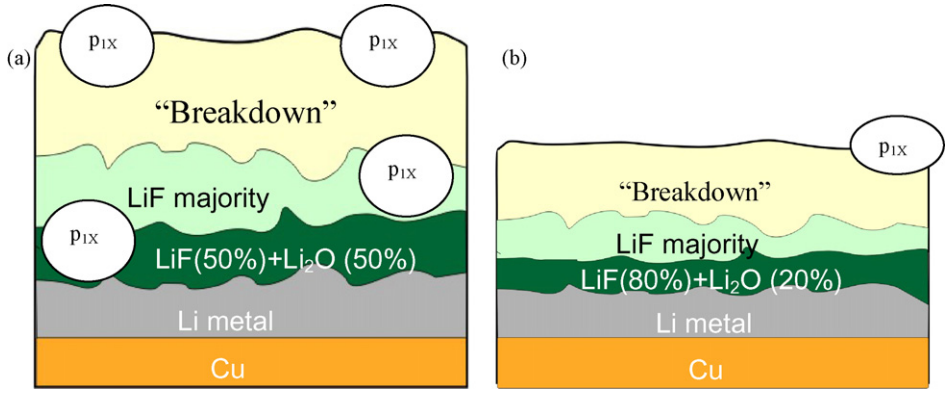


**Fig. 10.** A generalized schematic of SEI layer on Li metal (a-without zwitterion; b-with zwitterion). $P_{1X}$ refers to pyrrolidinium cation and related products. Breakdown refers to outer layer of electrolyte breakdown products. SEI developed in presence of a zwitterion is shown to be thinner and containing less breakdown products, consistent with XPS findings.

more extreme experiment given that the potential is immediately switched to lithium plating potentials, compared with a lithium surface which is covered by a native film.

## 5. Conclusions

The addition of 0.15 mol $kg^{-1}$ *N*-methyl-*N*-(butyl sulfonate) pyrrolidinium zwitterion to 0.5 mol $kg^{-1}$ Li[$NTf_2$]/[$C_3$mpyr][$NTf_2$] electrolyte is shown to have a considerable beneficial effect on the SEI formed on the lithium-metal surface. The improvement in the rate capability of symmetrical cells is clearly demonstrated to be largely dependent on the SEI thickness and conductance; it appears to be independent of the transport processes in the electrolyte. This suggests that the SEI properties are the dominant factor in controlling the rate capability of lithium devices employing $[NTf_2]^-$-based ionic liquids as electrolytes. This provides a clear path forward for the successful employment of ionic liquids as electrolytes in lithium-metal batteries.

## Acknowledgements

This work was supported financially by the Australian Research Council through the Centre of Excellence for Electromaterials Science. The authors gratefully acknowledge this support.

## References

[1] N. Munichandraiah, L.G. Scanlon, R.A. Marsh, J. Power Sources 72 (1998) 203–210.
[2] J.I. Yamaki, S.I. Tobishima, in: J.O. Besenhard (Ed.), HandBook of Battery Materials, Wiley–VCH, New York, 1999, pp. 339–357.
[3] S.B. Brummer, V.R. Koch, in: D.W. Murphy, J. Broadhead, B.C.H. Steel (Eds.), Materials for Advanced Batteries, Plenum, New York, 1980, pp. 123–143.
[4] J.I. Yamaki, S.I. Tobishima, Y. Sakurai, K.I. Saito, J. Hayashi, J. Appl. Electrochem. 28 (1997) 135–140.
[5] E. Peled, J. Electrochem. Soc. 126 (1979) 2047–2051.
[6] D. Aurbach, J. Power Sources 89 (2000) 206–218.
[7] E. Peled, D. Golodnitsky, in: P.B. Balbueria, Y. Wany (Eds.), SEI on Lithium, Graphite, Disordered Carbons and Tin-Based Alloys, World Scientific, South Carolina, 2003, Ch 1.
[8] E. Peled, D. Golodnitsky, J. Penciner, in: J.O. Besenhard (Ed.), HandBook of Battery Materials, Wiley–VCH, New York, 1999, pp. 419–456.
[9] J.R. Owen, Chem. Soc. Rev. 26 (1997) 259–268.
[10] P.C. Howlett, D.R. MacFarlane, A.F. Hollenkamp, J. Power Sources 114 (2003) 277–284.
[11] J.H. Shin, W.A. Henderson, S. Passerini, Electrochem. Commun. 5 (12) (2003) 1016–1020.
[12] H. Sakaebe, H. Matsumoto, Electrochem. Commun. 5 (7) (2003) 594–598.
[13] Y. Katayama, T. Morita, M. Yamagata, T. Miura, Electrochemistry (Tokyo Jpn.) 71 (2003) 1033–1035.
[14] R.D. Rogers, K.R. Seddon, Science 302 (2003) 792–793.
[15] F. Endres, T. Welton, in: P. Wasserscheid, T. Welton (Eds.), Ionic liquids in Synthesis, Wiley–VCH, Weinheim, Germany, 2003, pp. 289–318.
[16] K.R. Seddon, Nat. Mater. 2 (6) (2003) 363–365.
[17] E.B. Carter, S.L. Culver, P.A. Fox, R.D. Goode, I. Nati, M.D. Tickell, R.K. Traylor, N.W. Hoffman, J.H.J. Davis, Chem. Commun. 6 (2004) 630–631.
[18] T. Welton, Chem. Rev. 99 (8) (1999) 2071–2083.
[19] S. Zein El Abedin, F. Endres, in: R.D. Rogers, K.R. Seddon (Eds.), Ionic Liquids as Green Solvents, American Chemical Society, Washington, DC, 2003 (Ch. 36).
[20] P.C. Howlett, D.R. MacFarlane, A.F. Hollenkamp, Electrochem. Solid-State Lett. 7 (5) (2004) A97–A101.
[21] P.C. Howlett, E.I. Izgorodina, M. Forsyth, D.R. MacFarlane, Z. Phys. Chem. (Muenchen, Germany) 220 (2006) 1483–1498.
[22] C. Tiyapiboonchaiya, J.M. Pringle, J. Sun, N. Byrne, P.C. Howlett, D.R. MacFarlane, M. Forsyth, Nat. Mater. 3 (2004) 29–32.
[23] N. Byrne, P.C. Howlett, D.R. MacFarlane, M. Forsyth, Adv. Mater. (Weinheim, Germany) 17 (20) (2005) 2497–2501.
[24] P.C. Howlett, N. Brack, A.F. Hollenkamp, M. Forsyth, D.R. MacFarlane, J. Electrochem. Soc. 153 (3) (2006) A595–A606.
[25] N. Byrne, J. Efthimiadis, D.R. MacFarlane, M. Forsyth, J. Mater. Chem. 14 (1) (2004) 127–133.
[26] B.J. Meyer, N. Leifer, S. Sakamoto, S.G. Greenbaum, C.P. Grey, Electrochem. Solid-State Lett. 8 (3) (2005) A145–A148.
[27] V. Eshkenazi, E. Peled, L. Burstein, D. Golodnitsky, Solid State Ionics 170 (1–2) (2004) 83–91.
[28] M. Castriota, T. Caruso, R.G. Agostino, E. Cazzanelli, W.A. Henderson, S. Passerini, J. Phys. Chem. A 109 (2005) 92–96.
[29] D.R. MacFarlane, P. Meakin, J. Sun, N. Amini, M. Forsyth, J. Phys. Chem. B. 103 (1999) 4164–4170.